ACS Medicinal Chemistry Letters

Letter

pubs.acs.org/acsmedchemlett

Applications of Azo-Based Probes for Imaging Retinal Hypoxia

Md. Imam Uddin,[†] Stephanie M. Evans,[†] Jason R. Craft,[†] Lawrence J. Marnett,[§] Md. Jashim Uddin,*[,§] and Ashwath Jayagopal*[,†,‡]

[†]Department of Ophthalmology and Visual Sciences, Vanderbilt Eye Institute, Vanderbilt University Medical Center, Nashville, Tennessee 37232, United States

[‡]Molecular Physiology and Biophysics, Vanderbilt University School of Medicine, Nashville, Tennessee 37232, United States

[§]A. B. Hancock, Jr., Memorial Laboratory for Cancer Research, Department of Biochemistry, Chemistry and Pharmacology, Vanderbilt Institute of Chemical Biology, Center for Molecular Toxicology and Vanderbilt-Ingram Cancer Center, Vanderbilt University School of Medicine, Nashville, Tennessee 37232, United States

Supporting Information

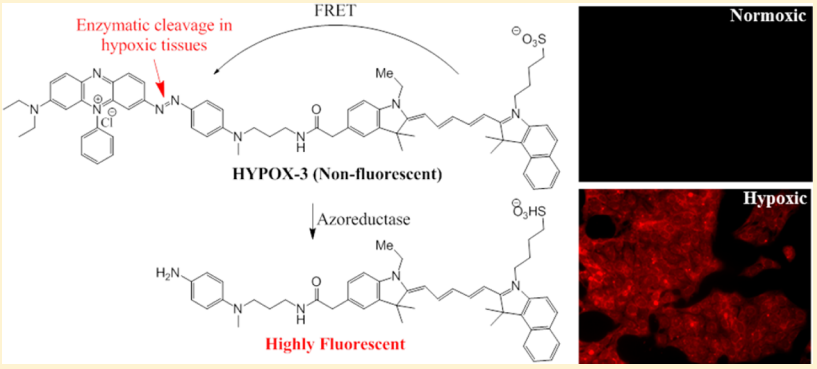

ABSTRACT: We report the design and synthesis of an activatable molecular imaging probe to detect hypoxia in mouse models of retinal vascular diseases. Hypoxia of the retina has been associated with the initiation and progression of blinding retinal vascular diseases including age-related macular degeneration, diabetic retinopathy, and retinopathy of prematurity. *In vivo* retinal imaging of hypoxia may be useful for early detection and timely treatment of retinal diseases. To achieve this goal, we synthesized HYPOX-3, a near-infrared (NIR) imaging agent coupled to a dark quencher, Black Hole Quencher 3 (BHQ3), which has been previously reported to contain a hypoxia-sensitive cleavable azo-bond. HYPOX-3 was cleaved in hypoxic retinal cell culture and animal models, enabling detection of hypoxia with high signal-to-noise ratios without acute toxicity. HYPOX-3 fluorescences in hypoxic cells and tissues and was undetectable under normoxia. These imaging agents are promising candidates for imaging retinal hypoxia in preclinical disease models and patients.

KEYWORDS: *Hypoxia, imaging agents, retina, retinal imaging, retinal hypoxia, molecular imaging*

INTRODUCTION

Retinal health is highly dependent on adequate supply of oxygen and nutrients to support metabolic processes critical for proper visual functions. An inadequate supply of oxygen may cause hypoxia involved in initiation and progression of blinding retinal vascular diseases, including diabetic retinopathy (DR), glaucoma, retinopathy of prematurity (ROP), and age-related macular degeneration (AMD).[1,2] A number of methods have been developed for the detection of retinal oxygen levels using retinal oximetry,[3] phosphorescence lifetime imaging,[4] and Doppler optical coherence tomography (OCT)[5] to understand the vascular oxygen supply and metabolism in the retina. However, these imaging approaches do not permit the direct identification of hypoxic cells in the retina. Though a number of methods have been reported in the literature to visualize hypoxia in tumor tissues using radioactive isotopes,[6,7] there is no practical noninvasive imaging technology available to detect hypoxia in retinal tissues.[8,9] Traditionally, technologies that are used for studying retinal hypoxia include Pimonidazole-mediated immunohistochemistry that is limited exclusively to an ex vivo method of examination.[10]

Recently, we described the development of optical imaging probes HYPOX-1 and HYPOX-2 based on nitroimidazoles conjugated to fluorescent dyes as sensitive imaging probes to detect hypoxia in mouse models of oxygen-induced retinopathy.[11] These fluorescein-based conjugates of 2-nitroimidazole accumulated within hypoxic cells in the retina and were subject to bioreduction by nitroreductases in hypoxic tissues, triggering intracellular adduct formation, and could detect the hypoxic tissues ex vivo.[11] It has been well established that hypoxia leads

Received: December 15, 2014
Accepted: February 12, 2015
Published: February 12, 2015

DOI: 10.1021/ml5005206
ACS Med. Chem. Lett. 2015, 6, 445−449

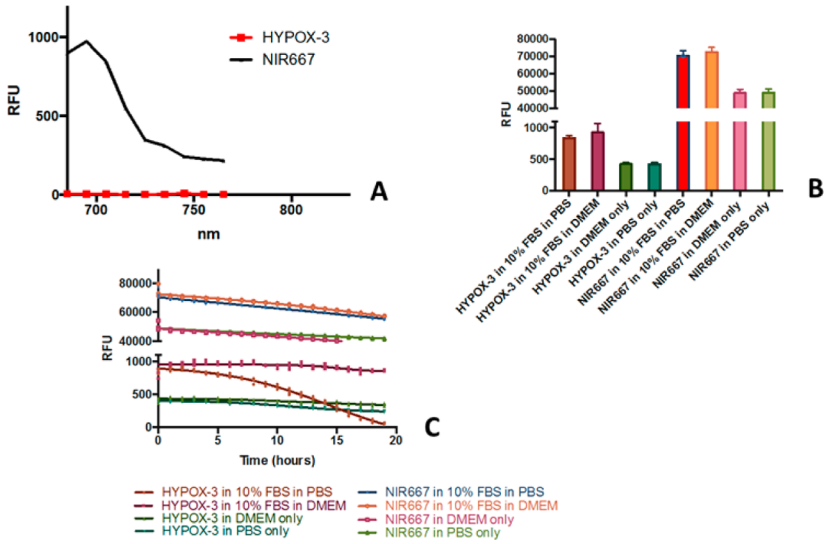

Figure 1. Fluorescence properties and stability of the HYPOX-3 probe in solution. (A) Fluorescence spectra of HYPOX-3 comparing with the parent NIR667 dye. (B) Stability of HYPOX-3 compared to NIR667 in serum containing medium. (C) Stability of HYPOX-3 and NIR667 in solution.

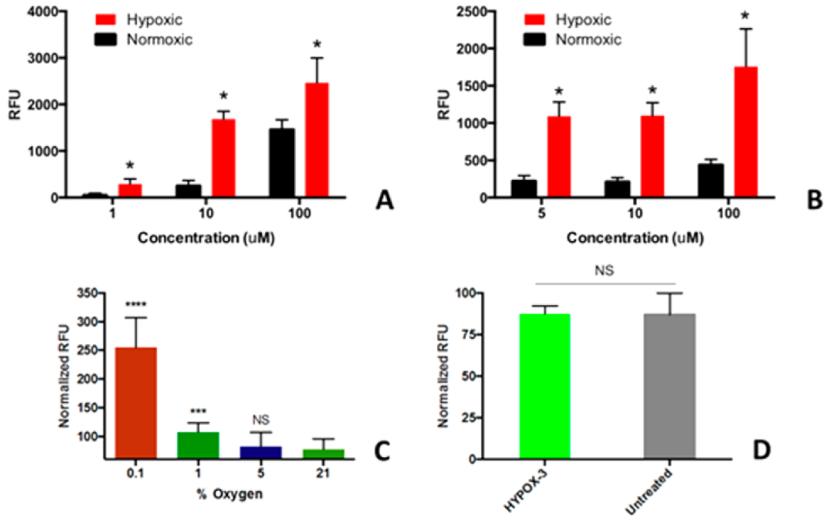

Figure 2. In vitro specificity, sensitivity, and toxicity of HYPOX-3 in retinal cell culture. (A–C) Concentration-dependent fluorescence enhancement of HYPOX-3 in hypoxic cells. (A) R28 cells were conditioned under hypoxia and normoxia treated with HYPOX-3 exhibited dose-dependent fluorescence enhancement in a microplate fluorescence spectrophotometric assay. (B) Human ARPE-19 cells showed similar fluorescence enhancement at hypoxic condition compared to normoxia. The hypoxic conditions were prepared by purging nitrogen/carbon dioxide gas for 5 min and then incubation for 4 h. The excitation and emission wavelengths were 670 and 704 nm, respectively. (C) Oxygen concentration-dependent fluorescence enhancement of HYPOX-3 (10 μM). Significant fluorescence signal enhancement was observed at 0.1% and 1% oxygen compared to the ambient oxygen level. (D) Nucview-488 activity was monitored under HYPOX-3 treated (10 μM) and untreated retinal R28 cells, and no changes in activity were observed. Statistical significances were evaluated using the nonparametric Wilcoxon Rank Sum (Mann–Whitney U) tests in GraphPad Prism 4; (n = 6) *p < 0.001, ***p = 0.0004, ****p < 0.0001. NS = not significant.

to reductive stress in retinopathy, which leads to increased expression of reductases including azoreductases and nitroreductases at the lesion.[12] Having developed fluorescence imaging agents that are retained in hypoxic cells via nitroreductases, we sought to compare these approaches with azoreductase-activatable imaging agents. Activatable imaging agents have the advantages of being optically quenched until dequenched by a molecular event, such as enzymatic cleavage[13−15] or reduction,[14] making them useful probes for imaging molecular processes with high signal-to-noise ratios.

Black Hole Quencher 3 (BHQ-3) is an efficient fluorescence quencher with near-infrared (NIR) dyes serving as acceptor in Förster resonance energy transfer (FRET) mechanism and features an azo-bond cleavable by azoreductases.[16] Nagano et. al showed that the azo-group of BHQ-3 could be used as the hypoxia-sensitive moiety in live cancer cells.[17] Furthermore, near-infrared (NIR) probes have several advantages for biological applications, including low phototoxitcity, low autofluorescence, and good tissue penetration abilities.[18] Building on this work, we developed a hypoxia-responsive imaging probe featuring a near-infrared (NIR) dye coupled to a hypoxia activatable BHQ-3 moiety and evaluated its utility for imaging retinal hypoxia. Established cell culture models and mouse models of hypoxia-associated retinal disease were

DOI: 10.1021/ml5005206
ACS Med. Chem. Lett. 2015, 6, 445−449

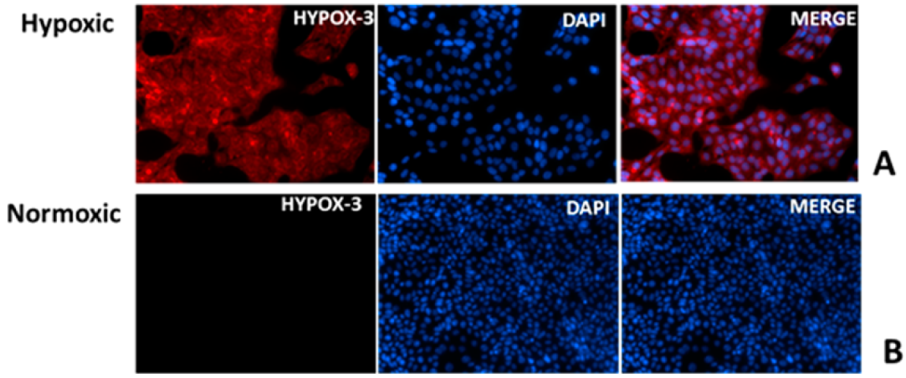

Figure 3. Fluorescence microscopy of R28 cells after incubating with HYPOX-3. Cells were treated with 10 μM HYPOX-3 and subjected to normoxia or hypoxia conditioning for 4 h. (A) Hypoxia-conditioned cells exhibited strong fluorescence and (B) normoxia-conditioned cells after treated with HYPOX-3 showed minimal fluorescence compared to hypoxic cells.

chosen to test the specificity of the imaging agents for hypoxic cells and in vivo imaging.

Synthesis of HYPOX-3 was carried out according to methods described in the Supporting Information and characterized using NMR and LRMS analysis (Supporting Figures S2−S3).

Native HYPOX-3 fluorescence was undetectable using fluorescence spectrophotometry (Figure 1A); this lack of fluorescence was not altered by incubation in serum (Figure 1B). HYPOX-3 possesses high photostability at room temperature in solution for at least 24 h as determined by kinetic fluorescence studies (Figure 1C). Next, to examine whether the new HYPOX-3 probe could detect hypoxia in biological systems, we first conducted an in vitro assay using retinal neuronal cells (R28) and human retinal pigment epithelial cell line (ARPE-19), which are sensitive to hypoxia. We previously confirmed that hypoxia was achieved in these retinal cell lines using qRT-PCR,[11] and the level of hypoxia was further confirmed by Pimonidazole immunostaining (Supporting Figure S1). An increase in the fluorescence intensity of HYPOX-3 was observed only under hypoxia after incubating for 4 h. The fluorescence intensity of the probe increased by 6.6-fold using a microplate fluorescence spectrophotometric assay (Figure 2A,B). The sensitivity of the probe was monitored under different oxygen concentrations and the fluorescence intensity was measured using a microplate fluorescence spectrophotometric assay. Statistically significant fluorescence enhancement was observed at 0.1% and 1% oxygen compared to higher, ambient oxygen levels (Figure 2C).

The safety of the HYPOX-3 component was confirmed as measured using a caspase-3 enzyme activity measurement assay to measure apoptosis. In this assay, HYPOX-3 was not acutely toxic toward R28 retinal neuronal cell lines (Figure 2D). Cells exposed to 10 μM HYPOX-3 showed no significant increase in Caspase-3 activity compared to untreated cells. Therefore, the dose appropriate for in vitro imaging appears to be well tolerated.

Microscopic fluorescence imaging of R28 cells incubated with HYPOX-3 further confirmed the specificity and selectivity of the probe. As demonstrated by representative images shown in Figure 3, HYPOX-3 was activated in hypoxic cells but not normoxic cells, which were also supported by the microplate assay. Under hypoxic conditions, an increase in fluorescence intensity was observed in R28 cells, whereas almost no fluorescence enhancement was seen under normoxia (Figure 3A,B). In vitro, HYPOX-3 exhibited optimal signal-to-noise ratios at a dose of 10 μM.

The mouse model of laser-induced choroidal neovascularization (LCNV) is used to model subretinal neovascular diseases such as neovascular or "wet" age related macular degeneration, and these models exhibit early hypoxia.[19] HYPOX-3 was administered to mouse models of LCNV and allowed it to circulate for 6 h. Imaging of retinal tissues following this circulation period revealed focal hypoxia within the LCNV lesion, but not in adjacent healthy vascularized retinal tissue (Figure 4A). Mice with normoxic retinas did not accumulate

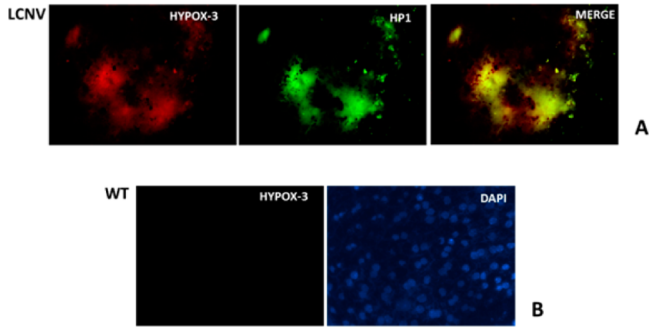

Figure 4. Ex vivo imaging of hypoxia in choroid-RPE flatmounts of the LCNV mouse model using HYPOX-3, which features colocalization of the immunostained Pimonidazole adducts with activated HYPOX-3. The fluorescence intensity was compared with a negative control WT choroid-RPE. (A) Colocalization of the activated HYPOX-3 (at 664 nm) with Pimonidazole adducts. (B) Minimal fluorescence activation of HYPOX-3 in a healthy control animal.

detectable amounts of HYPOX-3 as indicated by imaging studies using the same acquisition settings (Figure 4B). Therefore, HYPOX-3 activatable probes enable imaging of hypoxic retinal cells and tissues with high signal-to-noise ratios. Though similar probes have been published in the literature for the detection of hypoxia,[17] we have developed an alternative, more straightforward method for the synthesis of hypoxia detectable probe (HYPOX-3) with high chemical yield and fewer steps using commercially available materials with a short reaction sequence. We are currently designing instrumentation and protocols to enable visualization of in vivo administered HYPOX-3 and related probes in mouse models of retinal hypoxia.

In summary, we have demonstrated a facile route for the synthesis of an activatable hypoxia-sensitive imaging agent to detect level of hypoxia in retinopathy disorders. HYPOX-3 was

DOI: 10.1021/ml5005206
ACS Med. Chem. Lett. 2015, 6, 445−449

activated in hypoxic tissues, enabling fluorescence detection with high specificity and sensitivity using microscopy, and is compatible with in vivo retinal fluorescence imaging equipment. This approach is useful for elucidating the role of hypoxia in retinal diseases.

METHODS

Details of the synthesis of HYPOX-3 are described in the Supporting Information. NIR-667-carboxylic acid was obtained from Aldrich, and the dark quencher BHQ-3 amine was purchased from Biosearch Technologies (USA). Low glucose DMEM, DMEM/F12, Fetal Bovine Serum, GlutaMax, Gentamicin/Amphotericin B, and penicillin–streptomycin were obtained from GIBCO (USA). Human retinal pigment epithelial cell line (ARPE-19) was purchased from ATCC,[20] and rat retinal neuronal cell line R28[21] was purchased from KeraFast (MA, USA). A humidified cell culture chamber with ProOx 110 oxygen control device (BioSpherix Inc.) was configured for induction of hypoxia (0.1% O2) in mammalian cells according to published protocols.[11,22,23,23] A NucView 488 caspase 3 activity assay was from Biotium, Inc. A Hypoxyprobe immunodetection kit (antipimonidazole adduct antibody) was purchased from Hypoxyprobe, Inc. For immunofluorescence analysis of the hypoxia, secondary antirabbit antibody Alexa Fluor 488 (AF488) and Prolong Gold mounting media with DAPI were purchased from Life Technologies.

Animals. C57BL/6J female mice 4–6 weeks of age were purchased from Charles River Laboratories. All animal procedures used in this study were approved by the Vanderbilt University Institutional Animal Care and Use Committee and were performed in accordance with the ARVO Statement for the Use of Animals in Ophthalmic and Vision Research.

Retinal Cell Culture Conditions. ARPE-19 cells were cultured in DMEM/F12 supplemented with 10% Fetal Bovine Serum, 1× GlutaMAX, and 1× Gentamicin/Amphotericin B. R28 cells were cultured in low glucose DMEM supplemented with 10% Fetal Bovine Serum, 1× GlutaMAX, and 1× penicillin–streptomycin. Cells were maintained in a humidified environment with 5% CO_2 at 37 °C unless otherwise noted. Hypoxia was induced following our previously described method.[11] Briefly, cells were treated with HYPOX-3 diluted in complete media with up to 0.04% DMSO as cosolvent or Pimonidazole hydrochloride (100 μM) in complete medium, and the assay plates were placed into a humidified hypoxic chamber. Ambient air was displaced with a mixture of 5% CO_2 and 95% N_2 at a flow rate of 20 L/min for 5 min according to manufacturer instructions and published methods.[24] The chamber was clamped and placed at 37 °C for the remainder of the time point. R28 cells were treated with 100 μM Pimonidazole hydrochloride diluted in complete media and subjected to hypoxia or normoxia for 4 h.

In Vitro Cellular Activation of HYPOX-3 in Retinal Cells. ARPE-19 and R28 cells were seeded at a density of 20,000 and 15,000 cells per well, respectively, in a 96-well black plate with clear bottom. When cells were 90% confluent, they were treated with HYPOX-3 in complete media with 0.04% DMSO as cosolvent, and incubated under hypoxia or normoxia for 4 h. After incubation, both the cell cultures were washed 4 times with prewarmed Hank's Buffered Salt Solution (HBSS) and let sit for washout for an hour, then washed 4 more times with HBSS. Fluorescence intensity was read (absorbance, 670 nm; emission, 704 nm) using a Synergy Mx Plate Reader from Biotek.

In Vitro Toxicity Studies. A NucView-488 Caspase-3 activity measurement assay was performed on R28 cells. The assay was performed according to the manufacturer's instructions with the following specifications (Biotium, Inc.). Cells were seeded at 15,000 cells/well in a 96-well plate. HYPOX-3 imaging agent and vehicle control diluted in complete media were added and allowed to incubate for 4 h. After incubation, NucView-488 reagent was added at a concentration of 5 μM and fluorescence intensity was measured at 30 min (absorbance, 488 nm; emission, 520 nm) using a Synergy Mx Plate Reader (Biotek).

In Vitro Imaging of Retinal Cell Culture (R28) Using HYPOX-3. R28 cells were seeded at a density of 45,000 cells per well of 4-well chamber slides. When cells were 90% confluent, cells in 2 wells were treated with HYPOX-3 in complete media with 0.04% DMSO as cosolvent, and as control experiment, R28 cell in 1-well chamber was treated with Pimonidazole hydrochloride diluted in complete media, and then incubated under hypoxia or normoxia for 4 h. Cells were then washed 4 times in HBSS, fixed with 10% neutral buffered formalin (NBF) for 10 min at room temperature, washed 3 times with Tris buffered saline (TBS), and mounted with Prolong Gold with DAPI mounting media.

Ex Vivo Imaging of Hypoxia in LCNV Model Using HYPOX-3. In order to induce CNV by laser-induced ruptures of Burch's membrane in C57BL/6J female mice, an argon laser photocoagulator (Nidek AC-2000) mounted on a slit-lamp (Nidek SL-1600) was used to create four lesions in both the left and right eyes of each animal (100 μm spot size; 0.1 s duration; 0.1 W).[19,25–27] On day 2 post-laser injury, HYPOX-3 (60 mg/kg in PBS with DMSO as a cosolvent) was intraperitoneally injected. Six hours after the probe was incorporated, the mice were sacrificed, and the eyeballs were fixed in neutral buffered formalin (NBF). Hypoxyprobe was injected intraperitoneally at a concentration of 60 mg/kg body weight an hour before sacrifice of the animal. The eyeballs were harvested and kept in NBF for 30 min. The anterior segments and lenses were removed while dipping in NBF solution, and the remaining eye cups were mounted as described before.[11,28] Briefly, the choroid-sclera-RPE were fixed in NBF for 2 h and transferred in to Tris buffered saline (TBS) buffer before immunostaining. Tissues were then blocked/permeabilized in 10% donkey serum with 1% Triton X-100/0.05% Tween 20 in TBS for 6 h and were then stained for Pimonidazole adducts (Hypoxyprobe) followed by secondary antibody staining. The tissues were then mounted with Prolong Gold with DAPI mounting media. Images were taken using an epifluorescence microscope.

ASSOCIATED CONTENT

Supporting Information

Supplemental figures. This material is available free of charge via the Internet at http://pubs.acs.org.

AUTHOR INFORMATION

Corresponding Authors

*Phone: 615-343-7851. E-mail: ash.jayagopal@vanderbilt.edu.
*E-mail: jashim.uddin@vanderbilt.edu.

Author Contributions

The manuscript was written through contributions of all authors. All authors have given approval to the final version of the manuscript.

Funding

This work was supported by the National Institutes of Health (R01EY23397 (to A.J.), P30EY008126, U24DK059637, CA128323 (to M.J.U.), the American Diabetes Association (to A.J.), and Research to Prevent Blindness (Dolly Green Special Scholar Award (to A.J.) and Unrestricted Grant to Vanderbilt Eye Institute).

Notes

The authors declare no competing financial interest.

ACKNOWLEDGMENTS

Spectroscopic analysis was conducted in the Small Molecule NMR Facility and Mass Spectrometry Research Center at the Vanderbilt Institute of Chemical Biology.

REFERENCES

(1) Kaur, C.; Foulds, W. S.; Ling, E. A. Hypoxia-ischemia and retinal ganglion cell damage. *Clin. Ophthalmol.* **2008**, *2*, 879–889.
(2) Li, S. Y.; Fu, Z. J.; Lo, A. C. Hypoxia-induced oxidative stress in ischemic retinopathy. *Oxid. Med. Cell. Longevity* **2012**, *2012*, 426769.

DOI: 10.1021/ml5005206
ACS Med. Chem. Lett. 2015, 6, 445–449

(3) Hardarson, S. H.; Harris, A.; Karlsson, R. A.; Halldorsson, G. H.; Kagemann, L.; Rechtman, E.; Zoega, G. M.; Eysteinsson, T.; Benediktsson, J. A.; Thorsteinsson, A.; Jensen, P. K.; Beach, J.; Stefansson, E. Automatic retinal oximetry. *Invest. Ophthalmol. Vis. Sci.* **2006**, *47*, 5011−5016.
(4) Shahidi, M.; Shakoor, A.; Blair, N. P.; Mori, M.; Shonat, R. D. A method for chorioretinal oxygen tension measurement. *Curr. Eye Res.* **2006**, *31*, 357−366.
(5) Dai, C.; Liu, X.; Zhang, H. F.; Puliafito, C. A.; Jiao, S. Absolute retinal blood flow measurement with a dual-beam Doppler optical coherence tomography. *Invest. Ophthalmol. Vis. Sci.* **2013**, *54*, 7998−8003.
(6) Busk, M.; Jakobsen, S.; Horsman, M. R.; Mortensen, L. S.; Iversen, A. B.; Overgaard, J.; Nordsmark, M.; Ji, X.; Lee, D. Y.; Raleigh, J. R. PET imaging of tumor hypoxia using 18F-labeled Pimonidazole. *Acta Oncol.* **2013**, *52*, 1300−1307.
(7) Kizaka-Kondoh, S.; Konse-Nagasawa, H. Significance of nitroimidazole compounds and hypoxia-inducible factor-1 for imaging tumor hypoxia. *Cancer Sci.* **2009**, *100*, 1366−1373.
(8) Yang, Y.; Zhu, X. R.; Xu, Q. G.; Metcalfe, H.; Wang, Z. C.; Yang, J. K. Magnetic resonance imaging retinal oximetry: a quantitative physiological biomarker for early diabetic retinopathy? *Diabetic Med.* **2012**, *29*, 501−505.
(9) Scott, A.; Fruttiger, M. Oxygen-induced retinopathy: a model for vascular pathology in the retina. *Eye* **2010**, *24*, 416−421.
(10) Mowat, F. M.; Luhmann, U. F.; Smith, A. J.; Lange, C.; Duran, Y.; Harten, S.; Shukla, D.; Maxwell, P. H.; Ali, R. R.; Bainbridge, J. W. HIF-1alpha and HIF-2alpha are differentially activated in distinct cell populations in retinal ischaemia. *PLoS One* **2010**, *5*, e11103.
(11) Evans, S. M.; Kim, K.; Moore, C. E.; Uddin, M. I.; Capozzi, M. E.; Craft, J. R.; Sulikowski, G. A.; Jayagopal, A. Molecular probes for imaging of hypoxia in the retina. *Bioconjugate Chem.* **2014**, *25*, 2030−2037.
(12) Ross, D.; Beall, H. D.; Siegel, D.; Traver, R. D.; Gustafson, D. L. Enzymology of bioreductive drug activation. *Br J. Cancer Suppl.* **1996**, *27*, S1−8.
(13) Linder, K. E.; Metcalfe, E.; Nanjappan, P.; Arunachalam, T.; Ramos, K.; Skedzielewski, T. M.; Marinelli, E. R.; Tweedle, M. F.; Nunn, A. D.; Swenson, R. E. Synthesis, in vitro evaluation, and in vivo metabolism of fluor/quencher compounds containing IRDye 800CW and Black Hole Quencher-3 (BHQ-3). *Bioconjugate Chem.* **2011**, *22*, 1287−1297.
(14) Takahashi, S.; Piao, W.; Matsumura, Y.; Komatsu, T.; Ueno, T.; Terai, T.; Kamachi, T.; Kohno, M.; Nagano, T.; Hanaoka, K. Reversible off-on fluorescence probe for hypoxia and imaging of hypoxia-normoxia cycles in live cells. *J. Am. Chem. Soc.* **2012**, *134*, 19588−19591.
(15) Piao, W.; Tsuda, S.; Tanaka, Y.; Maeda, S.; Liu, F.; Takahashi, S.; Kushida, Y.; Komatsu, T.; Ueno, T.; Terai, T.; Nakazawa, T.; Uchiyama, M.; Morokuma, K.; Nagano, T.; Hanaoka, K. Development of azo-based fluorescent probes to detect different levels of hypoxia. *Angew. Chem., Int. Ed.* **2013**, *52*, 13028−13032.
(16) Myochin, T.; Hanaoka, K.; Komatsu, T.; Terai, T.; Nagano, T. Design strategy for a near-infrared fluorescence probe for matrix metalloproteinase utilizing highly cell permeable boron dipyrromethene. *J. Am. Chem. Soc.* **2012**, *134*, 13730−13737.
(17) Kiyose, K.; Hanaoka, K.; Oushiki, D.; Nakamura, T.; Kajimura, M.; Suematsu, M.; Nishimatsu, H.; Yamane, T.; Terai, T.; Hirata, Y.; Nagano, T. Hypoxia-sensitive fluorescent probes for in vivo real-time fluorescence imaging of acute ischemia. *J. Am. Chem. Soc.* **2010**, *132*, 15846−15848.
(18) Weissleder, R. A clearer vision for in vivo imaging. *Nat. Biotechnol.* **2001**, *19*, 316−317.
(19) Zhang, P.; Zhang, X.; Fan, J. L.; Hao, X. F.; Wang, Y. S.; Hui, Y. N.; Hu, D.; Zhou, J. Rac1 activates HIF-1 in laser induced choroidal neovascularization. *Int. J. Ophthalmol.* **2011**, *4*, 14−18.
(20) Dunn, K. C.; Aotaki-Keen, A. E.; Putkey, F. R.; Hjelmeland, L. M. ARPE-19, a human retinal pigment epithelial cell line with differentiated properties. *Exp. Eye Res.* **1996**, *62*, 155−169.
(21) Seigel, G. M.; Mutchler, A. L.; Adamus, G.; Imperato-Kalmar, E. L. Recoverin expression in the R28 retinal precursor cell line. *In Vitro Cell Dev Biol. Anim.* **1997**, *33*, 499−502.
(22) Genetos, D. C.; Cheung, W. K.; Decaris, M. L.; Leach, J. K. Oxygen tension modulates neurite outgrowth in PC12 cells through a mechanism involving HIF and VEGF. *J. Mol. Neurosci.* **2010**, *40*, 360−366.
(23) Yanni, S. E.; McCollum, G. W.; Penn, J. S. Genetic deletion of COX-2 diminishes VEGF production in mouse retinal Muller cells. *Exp. Eye Res.* **2010**, *91*, 34−41.
(24) Smith, L. E.; Wesolowski, E.; McLellan, A.; Kostyk, S. K.; D'Amato, R.; Sullivan, R.; D'Amore, P. A. Oxygen-induced retinopathy in the mouse. *Invest. Ophthalmol. Vis. Sci.* **1994**, *35*, 101−111.
(25) Shi, X.; Semkova, I.; Muther, P. S.; Dell, S.; Kociok, N.; Joussen, A. M. Inhibition of TNF-alpha reduces laser-induced choroidal neovascularization. *Exp. Eye Res.* **2006**, *83*, 1325−1334.
(26) Lu, H.; Lu, Q.; Gaddipati, S.; Kasetti, R. B.; Wang, W.; Pasparakis, M.; Kaplan, H. J.; Li, Q. IKK2 inhibition attenuates laser-induced choroidal neovascularization. *PLoS One* **2014**, *9*, e87530.
(27) Yang, X. M.; Wang, Y. S.; Zhang, J.; Li, Y.; Xu, J. F.; Zhu, J.; Zhao, W.; Chu, D. K.; Wiedemann, P. Role of PI3K/Akt and MEK/ERK in mediating hypoxia-induced expression of HIF-1alpha and VEGF in laser-induced rat choroidal neovascularization. *Invest. Ophthalmol. Vis. Sci.* **2009**, *50*, 1873−1879.
(28) Lambert, V.; Lecomte, J.; Hansen, S.; Blacher, S.; Gonzalez, M. L.; Struman, I.; Sounni, N. E.; Rozet, E.; de Tullio, P.; Foidart, J. M.; Rakic, J. M.; Noel, A. Laser-induced choroidal neovascularization model to study age-related macular degeneration in mice. *Nat. Protoc.* **2013**, *8*, 2197−2211.

DOI: 10.1021/ml5005206
ACS Med. Chem. Lett. 2015, 6, 445−449